

Numerical Modelling of Si sensors for HEP experiments and XFEL

Ajay K. Srivastava¹, D. Eckstein, E. Fretwurst, R. Klanner, G. Steinbrück

Institute for Experimental Physics, University of Hamburg, D-22761 Hamburg, Germany

E-mail: ajay.srivastava@desy.de

Abstract

Radiation damage is one major limitation for the use of silicon sensors in High Energy Physics and for research at synchrotron radiation sources and x-ray Free-Electron-Lasers. In this paper we describe the implementation of experimental results on radiation damage by neutrons and by 12 keV x-rays into the commercial simulation program Synopsys-TCAD and simulate the effects of radiation damage for two different sensor types and radiation fields:

- i) the dark current, the full depletion voltage and the electric field distribution for p^+n magnetic Czochralski Si pad sensors irradiated with neutrons, and
- ii) the electric field distribution and the breakdown voltage for x-ray irradiated n^+n FZ Si pixel sensors for the XFEL.

The simulations are part of a comprehensive program to optimize the design of silicon sensors with respect to radiation tolerance.

*9th International Conference on Large Scale Applications and Radiation Hardness of Semiconductor Detectors-Rd09
Florence, Italy
30 September - 2 October 2009*

¹ Speaker; work supported by the Helmholtz Alliance “Physics at the Terascale” and the European XFEL project

1. Introduction

Silicon sensors are widely used as precision tracking detectors at high energy colliders and as energy and position detectors in x-ray science. New accelerator facilities, like a possible luminosity upgrade of the Large Hadron Collider (LHC) to the Super-LHC (SLHC), aiming for a luminosity of $10^{35} \text{ cm}^{-2} \text{ s}^{-1}$, and the European x-ray Free-Electron-Laser (XFEL) pose new challenges with respect to radiation tolerance of silicon sensors. The maximum dose expected for 3 years of experimentation at the XFEL is 1 GGy of 12 keV photons.

Two main types of radiation damage occur in silicon sensors [1]:

- 1) *bulk damage*, caused by hadrons, resulting in a change of the effective doping concentration and thus of the full depletion voltage and the electric field distribution in the sensor, an increase in the leakage current due to generation-recombination centers, and a deterioration of the charge collection efficiency due to charge carrier trapping,
- 2) *surface damage*, mainly caused by x-rays, resulting in a build-up of bias dependent charges in the oxide (N_{ox}) and of traps at the Si-SiO₂-interface (N_{it}), causing bias dependent charge layers at the interface and surface generation currents (I_{ox}).

The detector laboratory of the Institute of Experimental Physics at Hamburg University is involved in a comprehensive program of radiation damage in silicon sensors with the elements: measurement of microscopic and macroscopic damage parameters, defect engineering, sensor simulation and measurement and simulation of signal shapes for different particle in the frame of the CERN RD50 collaboration [2], the Central European Consortium CEC of the CMS collaboration [3], the HGF-Alliance ‘Physics at the Terascale’ [4]. On the other hand our investigations on surface damage effects are part of the AGIPD collaboration [5] developing an Adaptive Gain Integrating Pixel Detector for the XFEL.

In the first part of the paper (section 2.1) we describe the implementation of experimental data on neutron induced defects in n-type Magnetic Czochralski (MCz) silicon into the commercial device simulation program Synopsys-TCAD [6]. Here we will present experimental results on the dark current and full depletion voltage in comparison to simulations, which include four radiation-induced defects [7, 8]. Special interest on n-type MCz silicon evolved from recent studies on damage effects in mixed radiation fields, i.e. irradiation by charged hadrons followed by neutron exposure [9]. The observed increase of the full depletion voltage is substantially lower compared to n- and p-type float zone (FZ) or p-type MCz Si material. This effect is due to a compensation of the positive space charge introduced by charged hadrons by the creation of negatively charged defects after neutron irradiation.

In the second part (section 2.2) the influence of surface damage effects induced by 12 keV x-rays on the static properties of a proposed n⁺n FZ Si pixel sensor for the application at the European XFEL is outlined. Here the relevant damage parameters (change of the fixed oxide charge N_{ox} , density of interface traps N_{it} (cm^{-2}) and the density of interface traps D_{it} ($\text{cm}^{-2} \text{ eV}^{-1}$)) were taken from experimental data [10, 11] and implemented into the Synopsys-TCAD

simulation program. Simulated distributions of the electric potential, electron density and electric field for a specific sensor layout and a given set of damage parameters will be presented and discussed.

2. Simulation and results

We use the Synopsys-TCAD device simulator. It solves Poisson's equation, the continuity, energy balance and lattice heat equations for holes and electrons. These equations describe the static and dynamic behaviour of carriers in semiconductors under the influence of external fields. The physical models used were Shockley–Read–Hall and Auger recombination, and field-dependent mobility. The impact ionization model is used to calculate the breakdown voltage of the sensor.

We use the following boundary conditions, constant potentials (Dirichlet at the contacts) and external field (Neumann at the SiO_2 surface and symmetry at the boundaries inside the sensor). For floating guard rings we impose a fixed potential and a null current flow on this contact. The potential of the floating contacts is found starting from an initial guess, using an iterative method.

2.1 Dark current field in $\text{p}^+\text{n}^-\text{n}^+$ MCz pad sensors

Radiation damage by energetic neutrons is dominated by the formation of clusters. Here we use “cluster” as a synonym for disordered regions with densely packed conglomerates of vacancies and/or interstitials. So far the knowledge on clusters is quite limited. Neither the structure and the constituents of the clusters nor their influence on the charge carrier capture characteristics are precisely known. Only recently clear evidences for the formation of electrically active extended defects were reported [7, 8, 12, 13]. These studies have revealed that there is a group of cluster-related defects with direct impact on the device performance, i.e. changes in the effective doping, which result in changes of the full depletion voltage, increase of the bulk generation current as well as the degradation of the charge collection efficiency due to charge carrier trapping.

To verify the proper implementation of the bulk damage parameters in the TCAD simulation we use data obtained from microscopic measurements of neutron irradiated p^+n MCz pad diodes manufactured by CiS [14] on 280 μm thick n-type MCz Si wafers having a resistivity of 873 Ωcm and an active area of 0.25 cm^2 . We derived a ‘four trap level model’ from microscopic measurements performed by means of the DLTS- (Deep Level Transient Spectroscopy) and the TSC-method (Thermally Stimulated Current) [7, 8, 13]. The defect parameters are summarized in table 1.

Here $E_{C,V}$ is the conduction and valance band energy, $\sigma_{n,p}$ the capture cross sections for electrons and holes, respectively, and η the introduction rate of the defects.. The main properties of the defects in table 1 are:

Table 1 Parameters of the ‘four trap level model’ for *n*-type MCz silicon.

Defect	Energy level [eV]	σ_n [cm ²]	σ_p [cm ²]	η [cm ⁻¹]
E5	E _C -0.46	3.0×10 ⁻¹⁵	4.1×10 ⁻¹⁵	12.4
H(152K)	E _V +0.42	3.05×10 ⁻¹³	1.0×10 ⁻¹³	0.06
C _i O _i	E _V +0.36	1.64×10 ⁻¹⁴	2.24×10 ⁻¹⁴	1.10
E(30K)	E _C -0.10	2.77×10 ⁻¹⁵	2.0×10 ⁻¹⁵	0.017

-E5 is a deep acceptor in the upper half of the band gap. It has been shown that this cluster related defect is mainly responsible for the radiation-induced increase of the dark current [8, 13]. The concentration of E5 as measured by DLTS does not reflect the real concentration because the trap cannot be totally filled with electrons due to potential barriers surrounding the disordered regions [15]. Therefore, the introduction rate has to be increased from 0.6 cm⁻¹ (DLTS value) to 12.4 cm⁻¹ in order to reproduce the measured dark current [16].

-H(152K) is a deep acceptor in the lower half of the band gap, negatively charged at room temperature [7, 8]. Thus, it is responsible for the increase of the negative space charge with increasing fluence, leading to type inversion by neutron irradiation [7, 17].

-E(30K) is a shallow donor in the upper half of the band gap [8]. It contributes to an increase of positive space charge and compensates partly the increase of the negative space charge introduced by the defect H(152K).

-The carbon-oxygen complex C_iO_i is a donor in the lower half of the band gap. This defect only contributes to the positive space charge if at room temperature the capture rate for holes is larger than the one for electrons in the space charge region [18].

The capture cross sections for the cluster related defects (E5, H(152K)) cannot be evaluated from DLTS or TSC measurements with sufficient accuracy. Therefore, we choose as a first guess values derived from charge carrier trapping measurements performed on neutron-irradiated sensors [19]. The cross sections σ_n and σ_p were finally tuned, to achieve agreement between simulation and experimental results for a device irradiated with 5×10¹³ n/cm².

Beside TCAD simulations with the ‘four trap level model’ the macroscopic device properties were also calculated using the relations given in [8, 20] resulting from Shockley-Read-Hall statistics:

$$N_{eff} = N_D + \sum n_T^{donor} - \sum n_T^{acceptor},$$

$$n_T^{donor, acceptor} = N_T^{donor, acceptor} \frac{e_{p,n}}{e_p + e_n} \quad (1)$$

where N_D is the initial doping concentration, n_T (*donor, acceptor*) the steady state occupancy of the defect levels, N_T the defect concentration. The emission rates $e_{p,n}$ for holes and electrons are given by:

$$e_{n,p} = c_{n,p} N_{C,V} \exp\left(\pm \frac{E_T - E_{C,V}}{k_b T}\right), \text{ with } c_{n,p} = \sigma_{n,p} v_{th,n,p} \quad (2)$$

$N_{C,V}$ is the effective density of states in the conduction/valance band, k_b the Boltzmann constant and $v_{th,n,p}$ the average thermal velocity of electrons/holes.

The reverse current at full depletion is given by:

$$I(V_{FD}) = q_0 A d \left(\sum e_n n_T^{acceptor} + \sum e_p n_T^{donor} \right) \approx q_0 A d \frac{n_i}{\tau_{g,eff}} \quad (3)$$

where q_0 is the elementary charge, A and d are the area and the thickness of the sensor, respectively, n_i is the intrinsic carrier concentration and $\tau_{g,eff}$ is the effective generation lifetime.

In Fig. 1 we compare the results of the TCAD-simulations and the calculations (eq(1)-eq(3)) based on the microscopic parameters to measured values of the full depletion voltage V_{FD} and the leakage current at full depletion $I_L(V_{FD})$ for three different neutron fluences [17].

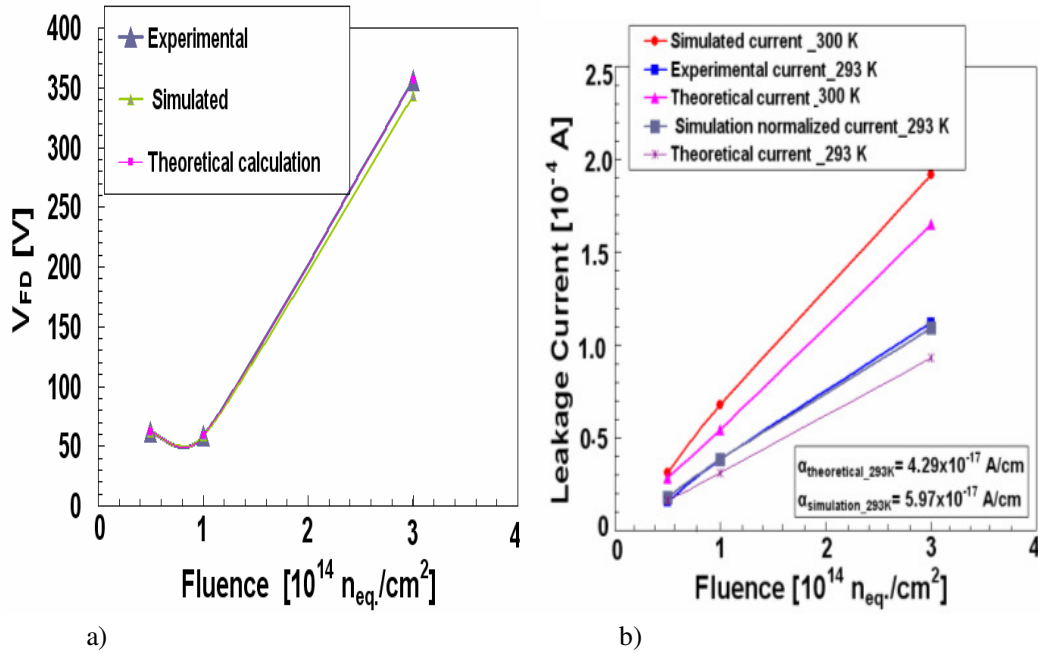


Figure 1 a) Full depletion voltage V_{FD} and b) Leakage current versus fluence for 280 μm thick p⁺n MCz Si pad sensors.

This comparison serves as a calibration for the damage model of neutron irradiated n-type MCz Si. For the fluence value of 5×10^{13} cm⁻² the space charge in the depleted device is still positive (not inverted) while for the larger fluences (1×10^{14} and 3×10^{14} cm⁻²) the material is inverted to p-type. After the adjustment of the damage parameters the simulation provides a good description of the measurements. The “theoretical calculations” based on Shockley-Read-Hall theory (see above) reproduce the values for V_{FD} but underestimate the measured leakage current $I_L(V_{FD})$. The underestimation might be due approximation in equation 1. The current related damage constant α at 293 K obtained from the simulation and measurements is 5.9×10^{-17} Acm⁻¹. It should be mentioned that this value is valid for as irradiated devices [Moll]. After short term annealing for 80 min at 60 °C the α value reduces to 4×10^{-17} Acm⁻¹.

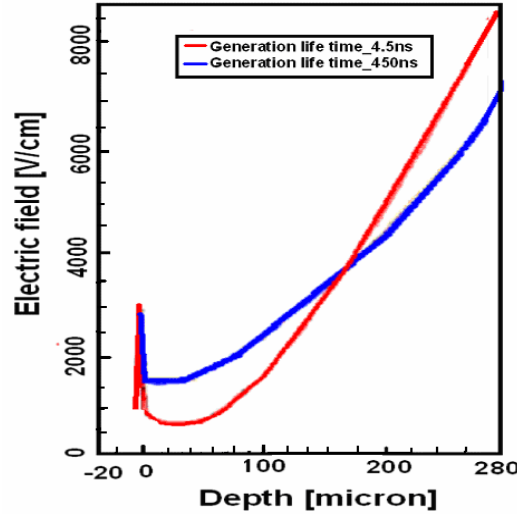


Figure 2 a) E-field versus depth (y) in a p^+n MCz Si pad sensor irradiated to $10^{14} n_{eq}$ for two values of the generation lifetime (double peak electric field).

The TCAD simulation also allows us to study the impact of deep traps on the spatial distribution of the electric field in the sensor. Fig. 2 shows two field distributions $E(y)$ across the sensor depth y (p^+ implant at $y = 0$) for two generation lifetimes of 4.5 ns and 450 ns. The applied reverse bias voltage 100 V is the same for both cases. The field distribution for the life time of 450 ns (blue line), as derived from eq.(3), corresponds to a fluence value of 10^{14} cm^{-2} . As can be seen from Fig. 2 the electric field as function of y is non-linear with a dominant increase of the field towards the n^+ back plane ($y=d$). Also at the p^+ electrode the field strength is larger compared to the region between 20 – 50 μm . Such a field distribution is typical for a highly irradiated and type-inverted device with maxima at both electrodes (so called double junction or “Double Peak” (DP) electric field). This effect is the result of a non-homogeneous occupancy of the deep traps due to the y -dependence of the thermally generated electron and hole densities responsible for the dark current [21]. For shorter generation lifetimes (larger current densities) the effect becomes more prominent as shown in Fig. 2 (red line, $\tau_g = 4.5$ ns).

2.2 Pixel sensors for the XFEL

At the European Free-Electron-Laser XFEL the sensors will be exposed to surface doses of up to 1 GGy of 12 keV x-rays. For this x-ray energy displacement damage effects can be excluded. I/V-, C/V- and TDRC- (Thermally Dielectric Relaxation Current)-measurements on gate controlled diodes and CMOS capacitors fabricated by CiS [14] on 2 k Ωcm n-type float zone (FZ) Si have shown that oxide charge density, interface trap density and surface generation velocity saturate, and even decrease beyond a dose of several MGy [11]. Based on the results at

5 MGy we use for the simulations an oxide charge density of $N_{ox} = 2 \times 10^{12} \text{ cm}^{-2}$ and two gaussian shaped interface trap level distributions with the parameters given in table 2.

Table 2 Parameters of the interface trap levels derived from measurements of gated diodes irradiated to 5 MGy. Given are the energy distance from the conduction band, the assumed rms width σ_{it} of the level and the trap density D_{it} .

type	Energy level [eV] $E_c - E_{it}$	σ_{it} [eV]	D_{it} [$\text{cm}^{-2} \text{ eV}^{-1}$]
acceptor	$E_c - 0.35$	0.05	4×10^{12}
acceptor	$E_c - 0.60$	0.05	4×10^{13}

At present the decision on the sensor layout (n^+n or p^+n) has not been taken. It is however clear, that 500 μm thick sensors are desirable to achieve a high detection efficiency for 12 keV x-rays. In addition, the sensors should be operated well above full depletion voltage, to control charge explosion (plasma) effects [22] at the expected high photon densities of 10^5 per $200 \times 200 \mu\text{m}^2$ pixel. Thus, the sensors should stand operating voltages of 1 kV for doses up to 1 GGy. These requirements (high voltage operation and minimizing plasma effects) favour the n^+n layout because collection of electrons is faster compared to that of holes.

As first step we have simulated the edge of the n^+n FZ Si pixel sensor. A schematic cross-section of the layout with 3 guard rings (GR1-GR3), 1 current ring (CR) and 1 current terminating ring (CTR) is shown in Fig.3a and the lateral dimensions (numbers in units of μm) at the p^+ side are presented in Fig. 3b.

A realistic simulation of the cut edge is difficult due to the high damage of the crystal structure which leads to a highly conductive layer. Therefore, the potential at the edge of the p^+ side will be the same as at the edge of the n^+ side which is at ground. The CTR is grounded and collects the major part of the current from the cut edge while the CR, which is also set to ground potential, collects only a small fraction of this current and part of the bulk current generated in this region. This design decouples the high leakage current from the active sensor volume.

The sensor material is n -type silicon with a doping concentration of $N_D = 10^{12} \text{ cm}^{-3}$ and has a thickness of 500 μm . The full depletion voltage is found to be 197 V. The x-rays enter through the non-segmented p^+ -contact (bottom) and the signals are collected on n^+ -pixels at the opposite side. The voltage drop occurs over the guard rings surrounding the p^+ -implant. Here we assume a linear voltage drop between the main p^+n junction and the p^+ current ring CR. Table 3 presents the most important parameters used in the simulation beside the interface trap parameters given in table 2.

Table 3 Main parameters for the simulated x-ray pixel sensors.

parameter	value
doping concentration (N_D)	$1 \times 10^{12} \text{ cm}^{-3}$
oxide+nitride thickness (t_{ox})	$0.4+0.1 \mu\text{m}$
p^+ junction depth (X_j)	$1 \mu\text{m}$
guard ring spacing (GS)	$42.5 \mu\text{m}$
guard ring width (GW)	$10 \mu\text{m}$
device thickness (W_N)	$500 \mu\text{m}$
n^+ implant junction depth	$5 \mu\text{m}$
metal-overhang width (W_{MO})	$5 \mu\text{m}$

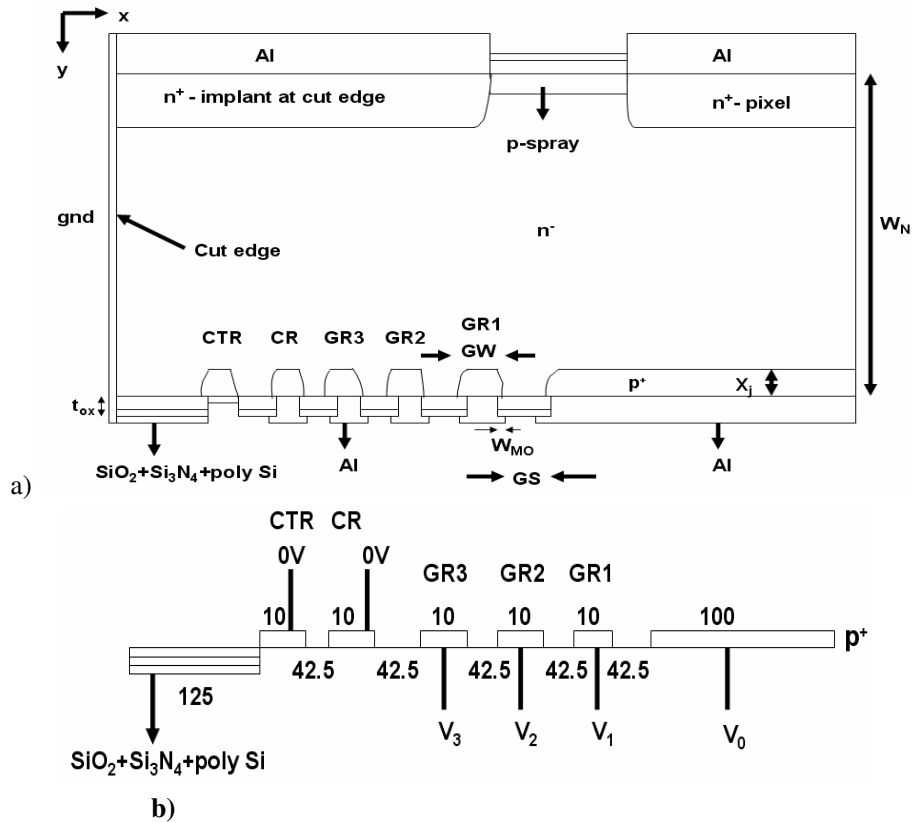
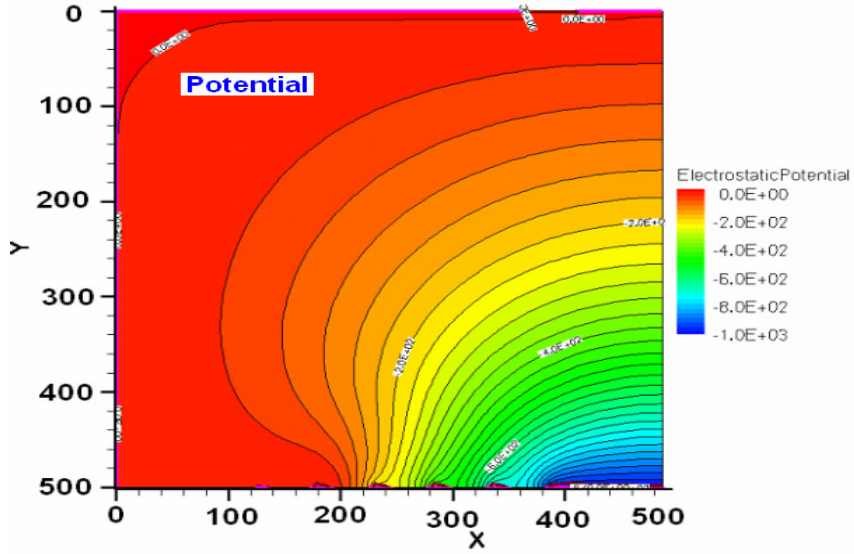


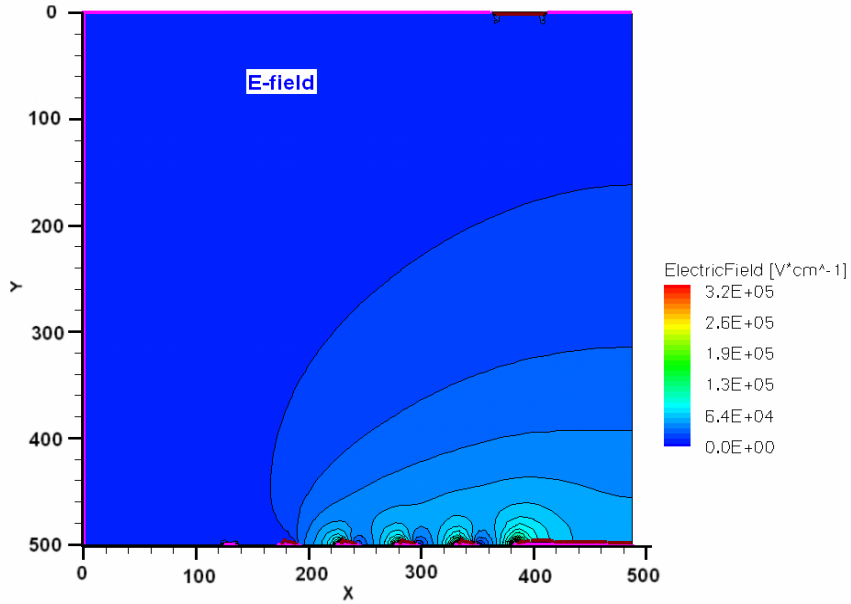
Figure 3 a) Schematic cross-section of n^+n FZ Si pixel sensor design b) Lateral dimensions in μm of the p^+ side of the pixel sensor simulated (V_0 : bias voltage, $V_1 = 0.75 \times V_0$, $V_2 = 0.5 \times V_0$ and $V_3 = 0.25 \times V_0$), CTR: Current terminating ring, CR: Current ring and GR: Guard ring.

Fig. 4 shows the results of the simulations, the electric potential (Fig. 4a), the electric field (Fig. 4b), the electron density (Fig. 4c), the surface electric field $0.5 \mu\text{m}$ below the SiO_2 -Si interface (Fig. 4d) and a zoomed view of the E-field near the curvature of the main p^+n junction (Fig. 4e). For the simulation the potentials of the 3 guard rings were kept at constant potential steps (see caption Fig. 3), the current ring (CR) at zero volt and the current terminating ring

(CTR) at the same potential. The bias voltage was applied to the main p⁺ contact and ramped up to 1 kV. Breakdown occurred at a voltage of 995 V. The maximum electric field is reached at the curvature of the main p⁺n junction (see Fig. 4e). It is noted, that the radiation induced acceptor traps at the SiO₂-Si interface partially compensate the effects of the oxide charges.



a)



b)

POS (RD09) 019

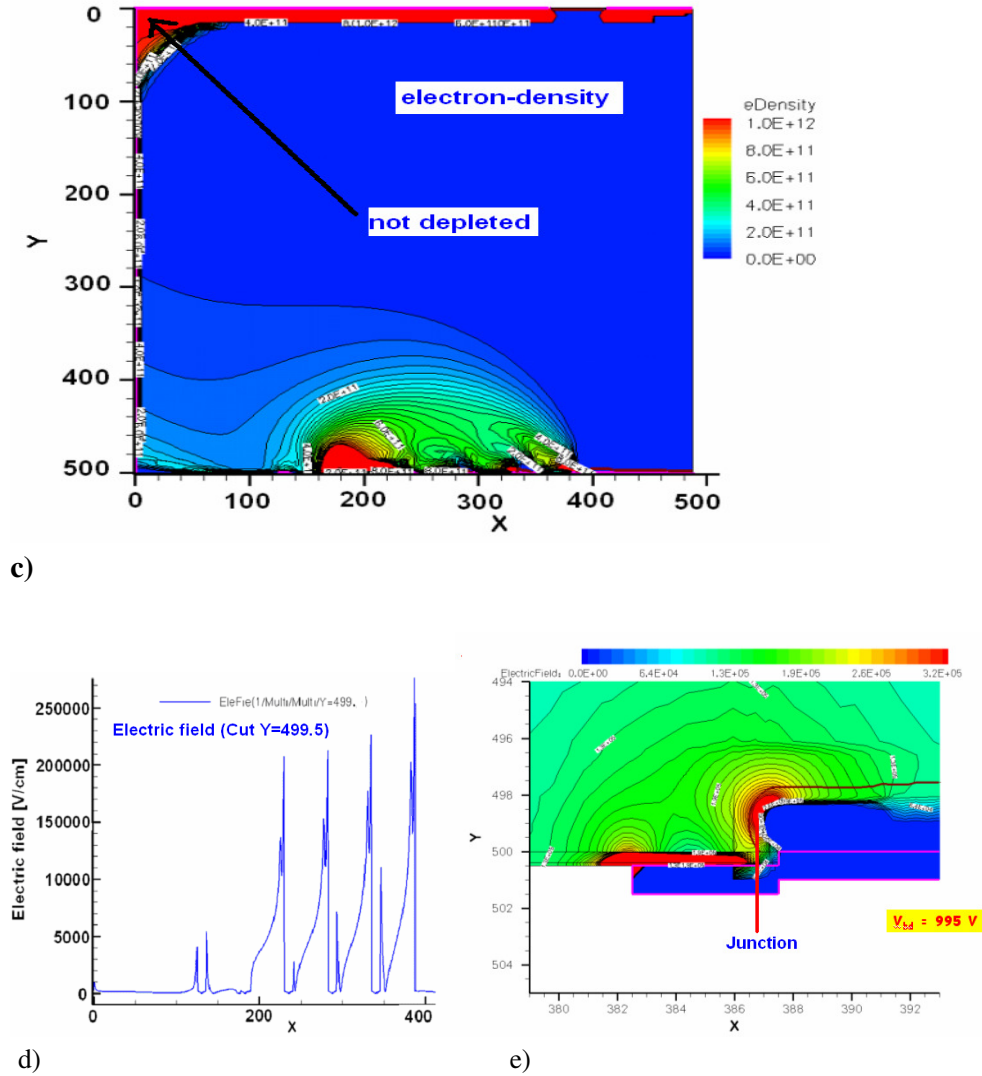


Fig. 4 Results of the simulation of the n^+n FZ Si pixel sensor a) Electrostatic potential, b) Electric field, c) Electron density, d) Surface electric field, 0.5 μm below the SiO_2 -Si interface, and (e) zoomed view of the E-field near to the p^+ curvature (breakdown region).

3. Summary and conclusions

For sensors irradiated with neutrons the simulations presented achieve a good description of the dose dependence of the dark current, the depletion voltage and the electric field distribution in the sensor. Next we will implement mixed (neutrons and energetic charged hadrons) irradiations and study the effects of charge carrier trapping.

For sensors irradiated with x-rays the simulation work has just started. On the other hand the AGIPD collaboration has not yet decided if the sensors will be of n - (n^+n) or of p - type (p^+n). The aim is to design a pixel sensor of 500 μm thicknesses, which is able to stand an

operating voltage of at least 1 kV to control charge explosion effects for x-ray doses between 0 and 1 GGy.

References

- [1] G. Lindström, “Radiation damage in silicon detectors”, Nucl. Instr. and Meth. A512 (2003) 30
- [2] RD50 collaboration, <http://rd50.web.cern.ch/rd50/>
- [3] CEC, Central European Consortium, collaboration for the upgrade of the CMS silicon tracker
- [4] Helmholtz Alliance ‘Physics at the Terascale’, <http://www.terascale.de/>
- [5] AGIPD (Adaptive Gain Integrating Pixel Detector), <http://hasylab.desy.de/instrumentation/detectors/projects/agipd/>
- [6] Synopsys Inc., TCAD software, <http://www.synopsys.com/Tools/TCAD/DeviceSimulation/>
- [7] I. Pintilie et al., “Cluster related hole trap with enhanced-field emission – the source for long term annealing in hadron irradiated Si diodes”, Appl. Phys. Lett. 92 (2008) 024101
- [8] I. Pintilie, G. Lindström, A. Junkes, E. Fretwurst, “Radiation-induced point- and cluster-related defects with strong impact on damage properties of silicon detectors”, Nucl. Instr. and Meth. A 611 (2009) 52-68
- [9] G. Kramberger, V. Cindro, I. Dolenc, I. Mandić, M. Mikž, M. Zavrtanik, “Performance of silicon pad detectors after mixed irradiations with neutrons and fast charged hadrons”, Nucl. Instr. and Meth. A 609 (2009) 142-148
- [10] E. Fretwurst, F. Januschek, R. Klanner, H. Perrey, I. Pintilie, F. Renn, “Study of the radiation hardness of silicon sensors for the XFEL”, poster presented at the Nucl. Sci. Symposium IEEE, Dresden 2008, Germany, Conf. record N30-400
- [11] E. Fretwurst, R. Klanner, H. Perry, I. Pintilie, T. Theedt, “Radiation damage studies for silicon sensors for the XFEL”, accepted for publication in Nucl. Instr. and Meth. A
- [12] R. M. Fleming, C. H. Seager, D. V. Lang, E. Bielejec, and J. M. Campbell, “A bistable divacancylike defect in silicon damage cascades”, J. Appl. Phys. 104 (2008) 083702
- [13] A. Junkes, D. Eckstein, I. Pintilie, L. Makarenko, E. Fretwurst, “Annealing study of a bistable cluster defect”, Nucl. Instr. and Meth. A 612 (2010) 525-529
- [14] CiS Institute for micro sensors and photovoltaics GmbH, 99099 Erfurt, Germany, <http://www.cismst.de/>
- [15] E. V. Monakhov, J. Wong-Leung, A. Yu. Kuznetsov, C. Jagadish, and B. G. Svensson, “Ion mass effect on vacancy-related deep levels in Si induced by ion implantation”, Phys. Rev. B, Vol. 65 (2002) 245201
- [16] M. Petasecca, F. Moscatelli, D. Passeri, G.U. Pignatelli, “ Numerical simulation of radiation damage effects in p-type and n-type FZ silicon detectors”, IEEE Trans. Nucl. Sci., VOL. 53, NO. 5 (2006) 2971-2976
- [17] E. Fretwurst et al., “Radiation damage studies on MCz and standard and oxygen enriched epitaxial silicon devices”, Nucl. Instr. and Meth. A 583 (2007) 58-63

- [18] M. Moll, "Radiation Damage in Silicon Particle Detectors - Microscopic Defects and Macroscopic Properties", PhD thesis, DESYTHESIS- 1999-040, (1999)
- [19] G. Kramberger, V. Cindro, I. Mandić, M. Mikůz, M. Zavrtanik, "Effective trapping time of electrons and holes in different silicon materials irradiated with neutrons, protons and pions", Nucl. Instr. and Meth. A 557 (2006) 528-536
- [20] P. Bräunlich in: "Thermally Stimulated Relaxation in Solids", editor P. Bräunlich, (Springer-Verlag Berlin 1979) Ch.1 pp. 1
- [21] E. Verbitskaya, V. Eremin, I. Ilyashenko, Z. Li, J. Härkönen, E. Tuovinen, P. Luukka, "Operation of heavily irradiated silicon detectors in non-depletion mode", Nucl. Instr. and Meth. A 557 (2006) 528-536
- [22] J. Becker, D. Eckstein, R. Klanner, G. Steinbrück, on behalf of the AGIPD Consortium, "Impact of plasma effects on the performance of silicon sensors at an X-ray FEL", Nucl. Instr. and Meth. A 615 issue2 (2010) 230-236